Simplified model to treat the electron attachment of complex molecules: Application to H_2CN and the quest for the CN^- formation mechanism

C. H. Yuen,[1] N. Douguet,[1] S. Fonseca dos Santos,[2] A. E. Orel,[3] and V. Kokoouline[1]
[1]*Department of Physics, University of Central Florida, Orlando, Florida 32816, USA*
[2]*Department of Physics, Rollins College, Winter Park, Florida 32789, USA*
[3]*Department of Chemical Engineering and Materials Science, University of California, Davis, California 95616, USA*

(Received 10 January 2019; published 1 March 2019)

We present a simplified approach to the dissociative electron attachment of polyatomic molecules. A reduced nuclear coordinate driving the dissociative process immediately following the resonance capture is introduced and allows an estimation of the cross section. The model is applied to the H_2CN molecule, which is considered as a precursor in the formation of the CN^- anion observed in the IRC +10216 carbon star. The computed rate coefficient suggests that the dissociative electron attachment of H_2CN may not be an efficient reaction to form CN^- in the circumstellar envelope of IRC +10216.

DOI: 10.1103/PhysRevA.99.032701

I. INTRODUCTION

The theoretical study of dissociative electron attachment (DEA) in large molecules is notoriously difficult due to the multidimensional nature of the problem. Because treatments of DEA in full dimensionality for complex systems is beyond current computational capabilities, a great deal of work has been conducted to unravel the underlying DEA mechanisms, e.g., by singling out one specific bond breaking, sorting out main dissociative pathways, or considering a subspace of coordinates [1–11]. Review of recent progress for DEA can be found in Ref. [12]. Only for a few triatomic systems, namely, HCN [13,14], ClCN, and BrCN [15], could a complete treatment be performed, while DEA for such "basic" triatomic molecules as H_2O [16–21] and CO_2 [22,23], where multiple electronic states of the target molecule and nonadiabatic couplings should be taken into account, are still actively studied, presenting a great deal of difficulty.

The formidable task of describing DEA in polyatomic molecules has often hindered the computation of DEA rate coefficients crucial for astrophysical models [24–26]. In fact, even an estimate of such rates is usually sufficient to understand the role played by specific reactions in the formation and destruction of molecules in the interstellar medium (ISM). Here, we propose a simplification of the computation of DEA cross sections by generalizing the model of O'Malley [27] and Bardsley [28] to systems with many coordinates in order to obtain an estimation of the resonant capture cross section. The model is applied on the DEA of H_2CN, which is closely related to the unsolved problem of CN^- formation in the ISM.

The density distribution of CN^- molecular anions observed in IRC +10216 [29] still puzzles physicists to date. Indeed, the carbon chains C_n^- and C_nH^- are considered to play a predominant role in the formation of CN^- upon collision with N atoms [30,31]; however, chemical models predict CN^- density produced by these reactions to peak in the outer region of the circumstellar envelope of IRC +10216 while the fitted density distribution peaks in the inner region [29].

This discrepancy suggests that reactions responsible for the CN^- production in the inner region of the envelope have been overlooked. Other than the reaction with C_n^- and C_nH^-, collision of HCN with H^- and radiative electron attachment (REA) of CN also produce CN^- in the inner region. In the chemical model used by Agúndez *et al.* [29], the temperature-independent Langevin rate of the former reaction was used and was shown to contribute less than 0.2% of the total amount of CN^-. This reaction has recently been studied by Satta *et al.* [32] using variational transition state theory. They found a strong temperature dependence on the rate coefficient and suggested that an extensive chemical model may produce CN^- more efficiently in the hotter inner region. In addition, a high density of H^- in the inner region could enhance this barrierless reaction. On the other hand, an *ab initio* calculation by Douguet *et al.* [33] found that the rate coefficient for formation of CN^- via REA is too slow to produce CN^- in the inner region.

In this article, we propose that a significant part of CN^- observed in the inner region originates from the DEA of the open-shell molecule H_2CN, i.e.,

$$\begin{aligned} H_2CN(X\,^2B_2) + e^- &\rightarrow (H_2CN)^{-*}(^1A_1) \\ &\rightarrow CN^-(X\,^1\Sigma^+) + H_2(X\,^1\Sigma_g^+) \\ &\rightarrow HCN(X\,^1\Sigma^+) + H^-(^1S), \end{aligned} \quad (1)$$

where the first and second dissociation channels are both exothermic by 1.92 and 0.6 eV, respectively. The H_2CN molecule was first detected in the cold dark molecular cloud TMC-1 in 1994 [34]. Soon after, Millar and Herbst proposed the existence of H_2CN in the circumstellar envelope of the carbon-rich star IRC +10216 by including the neutral-neutral reaction $N + CH_3 \rightarrow H_2CN + H$ in their chemical model [35,36].

Since the gas density in the ISM is low, open-shell species have a longer lifetime than in the laboratory. Therefore, if the rate coefficient for reaction (1) is fast enough, it could resolve

TABLE I. Calculated and experimental harmonic frequencies ω (in cm^{-1}) for each q. Our result is compared with the result from the CISD+Q/cc-pVTZ method [41]. Experimental frequencies are obtained from Ref. [42], except for ω_5, which is from Ref. [43].

	ω_1 CH_2 rock (B_2)	ω_2 Out of plane (B_1)	ω_3 CH_2 scissor (A_1)	ω_4 CN stretch (A_1)	ω_5 CH_2 sym stretch (A_1)	ω_6 CH_2 asym stretch (B_2)
This study	967.2	995.3	1420.6	1706.6	3080.0	3140.7
Ref. [41]	957.1	994.4	1401.6	1692.4	3031.9	3102.7
Experiment	912.8	954.1	1336.6	1725.4	2820	3103.2

the discrepancy of CN^- density between the chemical model and observation.

II. TARGET AND RESONANCE CALCULATION

We employ the MOLPRO suite of programs [37] to determine the electronic structure and vibrational frequencies of H_2CN. We first perform the calculation using multireference configuration interaction (MRCI) [38,39] with Hartree-Fock (HF) orbitals. The basis set for all atoms is chosen to be cc-pVQZ [40]. In the MRCI calculation, the $1s$ and $2s$ carbon and nitrogen core orbitals are frozen and we include eight active orbitals in the complete active space. At the equilibrium geometry, the bond lengths CH, NH, and the HCH angle are found to be 1.088 Å, 1.246 Å, and 121.1°, respectively. H_2CN at the equilibrium possesses C_{2v} point-group symmetry, with the ground-state electronic configuration

$$X^2B_2 : 1a_1^2 2a_1^2 3a_1^2 4a_1^2 1b_2^2 5a_1^2 1b_1^2 2b_2.$$

We then computed the harmonic frequencies and compared with theoretical [41,44–48] and experimental studies available in the literature [42,43]. In Table I we compare our results with Ref. [41] and the experimental studies [42,43]. We observe a good agreement between our results and the calculations [42] and only small discrepancies with the experimental results. We will use normal coordinates in the present study.

To compute the resonance position $\Delta(\vec{q})$ and width $\Gamma(\vec{q})$ at a given molecular geometry $\vec{q}$, we use the UK R-matrix code [49,50] in the QUANTEMOL-N suite [51] for electron-molecule scattering to obtain the R matrix. To be consistent with the MOLPRO calculation, we use a complete active space configuration interaction (CASCI) model to compute the electronic structure of the target using the same basis set, molecular orbitals, number of frozen orbitals, and complete active space. Eigenphase sums are fitted to the Breit-Wigner form, providing resonance energies and widths [52]. At electron energy below 5 eV and at H_2CN equilibrium geometry, we found three shape resonances; $^1A_1$ ($\Delta = 0.277$ eV, $\Gamma = 8.24$ meV), $^3A_2$ ($\Delta = 2.56$ eV, $\Gamma = 1.2$ eV), and $^1A_2$ ($\Delta = 3.15$ eV, $\Gamma = 1.49$ eV).

Figure 1 displays the eigenphase sum obtained from the static exchange model and the CASCI model for total symmetry $^1A_1$, $^3A_2$, and $^1A_2$. Since H_2CN has large polarizability $\boldsymbol{\alpha}$, the static exchange model neglects a substantial gain of kinetic energy of electrons from the $-\boldsymbol{\alpha}\cdot\boldsymbol{r}/2r^5$ potential, with $\boldsymbol{\alpha} \approx 1.33\ a_0^3\,\hat{r}$. Therefore, the positions of resonances from the static exchange model are at higher energies than the CASCI model. Nevertheless, the fact that those three resonances are seen in the static exchange model implies that all the resonances are shape resonances.

A similar R-matrix calculation was reported by Wang *et al.* [53], who also found the $^3A_2$ and $^1A_2$ shape resonance at similar positions but with widths 2 orders smaller than our results. Moreover, they did not find the $^1A_1$ shape resonance at low energy, most likely because they used a relatively small basis set. We have ascertained that the position and width of the lowest resonance remain relatively stable with respect to the variation of the size of the R-matrix box, the size of the complete active space, and the basis set.

Analyzing the symmetry, one can deduce the possible dissociation products from certain resonance states. For the two dissociation channels in (1), the total spin of the system is zero so that resonance in the triplet state cannot lead to dissociation. To dissociate into $CN^-(X^1\Sigma^+) + H_2(X^1\Sigma_g^+)$ or $HCN(X^1\Sigma^+) + H^-(^1S)$, the system must be symmetric with respect to reflection on the plane spanned by $CN^- + H_2$ or $HCN + H^-$. However, upon symmetry breaking, $^1A_2$ becomes the $^1A''$ irreducible representation in the C_s group, such that it is antisymmetric with respect to such reflection. Therefore, only the $^1A_1$ resonance could lead to dissociation to either of the two channels.

Inspection of the continuum wave function shows that the partial waves of the scattering electron contributing to the $^1A_1$ resonance transform as the B_2 irreducible representation, as expected, because the electronic state of the target is B_2.

Figure 2 shows the resonance energies $\Delta(\vec{q})$ for different normal-mode displacements. Because certain normal modes reduce C_{2v} symmetry to C_s symmetry, the total electronic

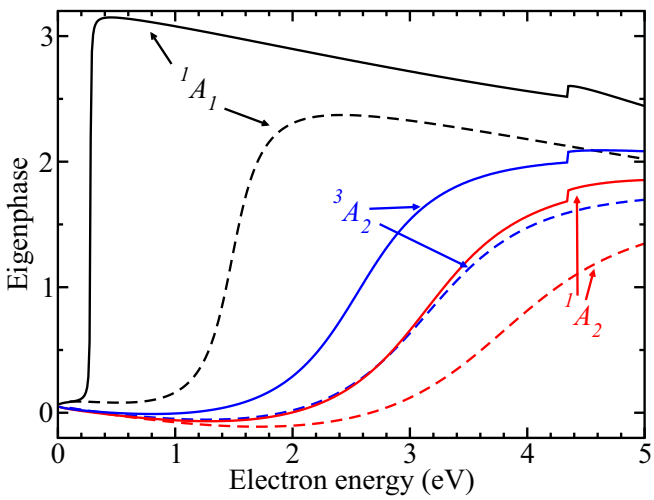

FIG. 1. The scattering eigenphase sum for total symmetry $^1A_1$, $^3A_2$, and $^1A_2$. The solid and dashed lines are the results obtained from the CASCI model and the static exchange model, respectively.

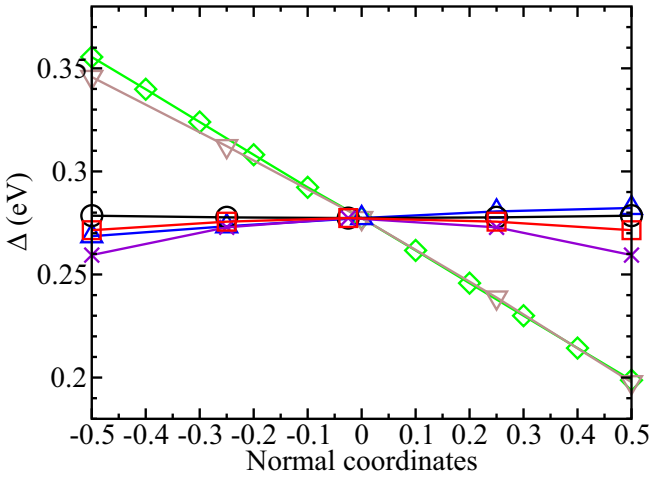

FIG. 2. The variation of resonance energies $\Delta(\vec{q})$ (in eV) over q_1 (black circles), q_2 (red squares), q_3 (green diamonds), q_4 (blue triangles up), q_5 (brown triangles down), and q_6 (violet crosses) for H_2CN.

wave function with such normal displacements of the nuclei is represented in a different symmetry group, which introduces an uncertainty in the position and width of the resonance. Indeed, the resonance energies for the normal modes with C_s symmetry are found to differ from the ones with C_{2v} symmetry by about 25% near the equilibrium geometry. This is within the relative errors of resonance energies obtained from different basis sets and complete active space. To improve visualization, we manually shifted up the resonance energies for q_1, q_2, and q_6. For symmetry reasons, the resonance energies depend at least quadratically on the normal displacements q_1, q_2, and q_6 near the equilibrium. One the other hand, we observe a strong linear variation of Δ over q_3 and q_5, which suggests that these coordinates are the most relevant for electron capture. Of course, the latter vibrational motions are coupled on the resonance energy surface, and the system should follow the steepest descent of the resonance energy for stabilization such that we can regard the nuclei moving initially in a one-dimensional space near the capture region. Note that such an analysis can in general be extended to other systems.

Following electron capture, the system may reach some branching points on the anionic potential energy surface and eventually dissociate. Alternatively, the anionic transient could emit an electron (autodetachment) or radiatively cool towards lower vibrational states. To unravel the wave-packet dynamics, the potential energy surface of the $^1A_1$ electronic ground state of H_2CN^- would need to be explored in full dimensionality. Such a study, however, is out of scope of the present work, where we focus instead on presenting a simple model to describe the initial electron capturing step and thus obtain the upper bound to the DEA cross section.

III. THEORY OF RESONANT CAPTURE

In order to find the steepest descent or capture coordinate, we seek an orthogonal matrix which transforms (q_3, q_5) to (s_1, s_2):

$$\begin{pmatrix} \alpha & \beta \\ -\beta & \alpha \end{pmatrix} \begin{pmatrix} q_3 \\ q_5 \end{pmatrix} = \begin{pmatrix} s_1 \\ s_2 \end{pmatrix}. \tag{2}$$

Choosing s_1 as the capture coordinate leads to

$$\frac{\partial \Delta}{\partial s_1} = \alpha \frac{\partial \Delta}{\partial q_3} + \beta \frac{\partial \Delta}{\partial q_5}, \tag{3}$$

where the constants α and β are

$$\alpha = \frac{|\partial \Delta/\partial q_3|}{\sqrt{(\partial \Delta/\partial q_3)^2 + (\partial \Delta/\partial q_5)^2}}; \quad \beta = \sqrt{1-\alpha^2}.$$

Since the width of the resonance is narrow, we neglect the explicit energy dependence of the width, i.e., we only consider the on-shell width. In the so-called local complex potential approach [27,54,55], the metastable state ξ_d becomes the solution of the following equations:

$$\left[\hat{T} + U_d(\vec{q}) - \frac{i\Gamma(\vec{q})}{2} - E\right]\xi_d(\vec{q}) = V_d(\vec{q})\zeta(\vec{q}), \tag{4}$$

$$V_d(\vec{q}) = \sqrt{\frac{\Gamma(\vec{q})}{2\pi}}, \tag{5}$$

where $\hat{T}$ is the nuclei kinetic energy operator, U_d is the resonance energy plus the neutral potential energy, and ζ is the ground vibrational wave function of the target.

In our model, only the coordinates q_3 and q_5 participate in the capture process. Thus, in the spirit of the sudden approximation, we write the nuclei wave function ξ_d as

$$\xi_d(\vec{q}) \approx \xi_c(q_3, q_5)\chi(\vec{q'}), \tag{6}$$

where $\vec{q'}$ collects all the spectator coordinates and $\chi(\vec{q'})$ is the product of vibrational wave functions in the spectator coordinates. Similarly, we express the vibrational wave function of the target as

$$\zeta(\vec{q}) = \zeta_c(q_3, q_5)\chi(\vec{q'}). \tag{7}$$

We further express

$$\hat{T} = -\frac{\hbar\omega_3}{2}\frac{\partial^2}{\partial q_3^2} - \frac{\hbar\omega_5}{2}\frac{\partial^2}{\partial q_5^2} + \hat{T}_{\rm spec}, \tag{8}$$

$$\hat{T}_{\rm spec} = -\sum_{i'} \frac{\hbar\omega_{i'}}{2}\frac{\partial^2}{\partial q_{i'}^2}, \tag{9}$$

and

$$U_d(\vec{q}) = U_n(q_3) + U_n(q_5) + \Delta(\vec{q}) + U_{\rm spec}(\vec{q'}), \tag{10}$$

$$U_{\rm spec}(\vec{q'}) = \textstyle\sum_{i'} U_n(q_{i'}), \tag{11}$$

where U_n are the neutral potential energies, and the summation on i' runs over all spectator coordinates. Note that $\chi(\vec{q'})$ is the eigenfunction of $\hat{T}_{\rm spec} + U_{\rm spec}$ with the eigenvalue equals to the sum of zero-point energies of all spectator coordinates.

Next, multiplying $\chi(\vec{q'})$ on the left in Eq. (5) and integrating over $\vec{q'}$, we obtain the two-dimensional equation in

dimensionless coordinates,

$$\left[-\frac{\hbar\omega_3}{2}\frac{\partial^2}{\partial q_3^2} - \frac{\hbar\omega_5}{2}\frac{\partial^2}{\partial q_5^2} + U_n(q_3) + U_n(q_5) + \Delta(q_3, q_5, \vec{0}) - \frac{i\Gamma(q_3, q_5, \vec{0})}{2} - E \right] \xi_d(q_3, q_5) = V_d(q_3, q_5, \vec{0})\zeta_c(q_3, q_5), \quad (12)$$

where we approximate the integrals of resonance energy and width with χ^2 over spectator coordinates at the resonance energy and width at $\vec{q'} = 0$.

Transforming (q_3, q_5) to (s_1, s_2), we then obtain

$$\left[\hat{T}_s + U_d(s_1, s_2) - \frac{i\Gamma(s_1, s_2)}{2} - E \right] \xi_d(s_1, s_2) = V_d(s_1, s_2)\zeta_c(s_1, s_2), \quad (13)$$

where the operator $\hat{T}_s$ is given by

$$\hat{T}_s = -\frac{\hbar\tilde{\omega}_1}{2}\frac{\partial^2}{\partial s_1^2} - \frac{\hbar\tilde{\omega}_2}{2}\frac{\partial^2}{\partial s_2^2} - \hbar\alpha\beta(\omega_5 - \omega_3)\frac{\partial^2}{\partial s_1 \partial s_2}, \quad (14)$$

while the potential U_d takes the form

$$U_d(s_1, s_2) = \tfrac{1}{2}\hbar\tilde{\omega}_1 s_1^2 + \tfrac{1}{2}\hbar\tilde{\omega}_2 s_2^2 + \Delta(s_1, s_2) + \hbar\alpha\beta(\omega_5 - \omega_3)s_1 s_2, \quad (15)$$

with

$$\tilde{\omega}_1 = \alpha^2\omega_3 + \beta^2\omega_5,$$

$$\tilde{\omega}_2 = \beta^2\omega_3 + \alpha^2\omega_5,$$

$$\zeta_c(s_1, s_2) = \zeta_c(q_3, q_5) = \frac{1}{\sqrt{\pi}} \exp\left[-\left(s_1^2 + s_2^2\right)/2 \right].$$

Denoting $\zeta_i(s_i) \equiv \pi^{-1/4} \exp(-s_i^2/2)$, we apply the sudden approximation again and have $\xi_d(s_1, s_2) \approx \xi_1(s_1)\zeta_2(s_2)$. Multiplying $\zeta_2(s_2)$ on both sides and integrating, we finally arrive at

$$\left[\frac{-\hbar\tilde{\omega}_1}{2}\frac{d^2}{ds_1^2} + U_d(s_1, 0) - \frac{i\Gamma(s_1, 0)}{2} - E \right] \xi_1(s_1) = V_d(s_1, 0)\zeta_1(s_1), \quad (16)$$

$$U_d(s_1, 0) = \frac{1}{2}\hbar\tilde{\omega}_1 s_1^2 + \Delta(s_1, 0), \quad (17)$$

where the cross terms of s_1 and s_2 vanish as $\zeta_2(s_2)$ is an even function. The energy E is the sum of zero-point energy of s_1 and energy of the scattering electron ε.

Finally, following the WKB approach by O'Malley [27] or Bardsley [28] and assuming the survival probability of the complex is unity, the capture cross section is given by

$$\sigma_{\text{cap}}(\varepsilon) = g\frac{2\pi^2}{k^2}\frac{\Gamma(s_\varepsilon)}{|U_d'(s_E)|}|\zeta_1(s_E)|^2, \quad (18)$$

where g is the ratio of statistical weight of product to reactant, and the classical turning point s_E and Frank-Condon point s_ε are obtained by solving $U_d(s_E) = E$ and $\Delta(s_\varepsilon) = \varepsilon$, respectively. We abbreviate $U_d(s_1, 0)$ and $\Gamma(s_1, 0)$ as $U_d(s_1)$ and $\Gamma(s1)$. The statistical weight for the product $H_2 + CN^-$ ($X^1\Sigma_g^+ \otimes X^1\Sigma^+$) is 1, while for the reactant H_2CN ($^2B_2$) it is 2, such that $g = 1/2$.

IV. RESULTS AND DISCUSSION

Figure 3 displays the resonance energy, anionic and neutral potential energies as functions of the capture coordinate s_1. The red line shows the first-order approximation of $\Delta(s_1)$,

$$\Delta(s_1) \approx \Delta(0) + \frac{d\Delta}{ds_1}(0)s_1,$$

which is seen to agree well with the data points for $-1 < s_1 < 1$. The blue dashed line is obtained by adding the resonance energy to the neutral potential energy. However, we note that as the electronic wave function of the neutral target may not be well represented with the limiting complete active space, the minimum of the anionic potential energy is above the neutral, in contradiction to the photodetachment experiment [43]. In order to obtain the correct electron affinity, we use the *ab initio* data obtained from RCCSD(T)/aug-cc-pVQZ [45] and shift the anionic potential energy down by 0.65 eV, which is shown as a blue solid line. Since there is a local minimum for the anion potential, it suggests that there is at least one barrier in the dissociation pathway to $CN^- + H_2$ or $HCN + H^-$. In our simplified model, we assume that the barrier height is smaller than 0.6 eV, such that there is no reflection of the outgoing flux from the barrier and the complex will eventually dissociate without autodetachment. At zero electron energy, the classical turning point s_E is around –1.4, such that the capture process occurs in a well-defined region of normal coordinates, thereby justifying our approach.

Figure 4 shows the effective width against effective resonance energy $\Delta(s_\varepsilon)$, which is equal to electron energy ε in this approach so as to enforce the threshold behavior [55]. The electronic structure calculations give the value $0.957\,ea_0$ for the permanent dipole moment of H_2CN as at $s_1 = 1.25$. This value of s_1 is only 0.04 a_0 away from the crossing point of the original anionic and neutral potential energy curves (blue dashed and black curves in Fig. 3). Since s-wave scattering is forbidden by symmetry, an estimation of the off-diagonal element of the dipole moment between p, d, and f partial

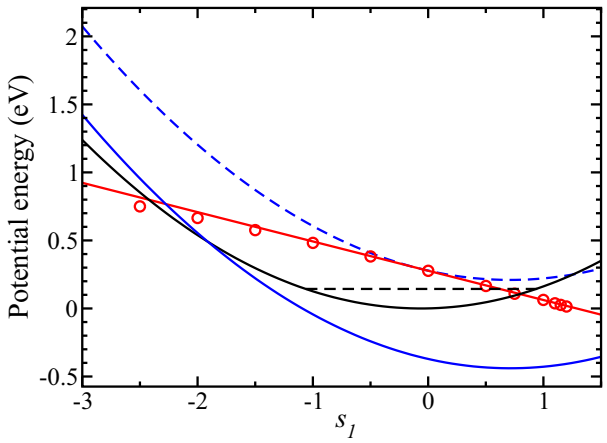

FIG. 3. The anionic potential energy U_d (blue dashed line), neutral potential energy U_n (black line), and resonance energy Δ (circles) and its linear approximation (red straight line) along s_1 for H_2CN at $s_2 = 0$. The black dashed line is the zero-point energy of the nuclei for coordinate s_1.

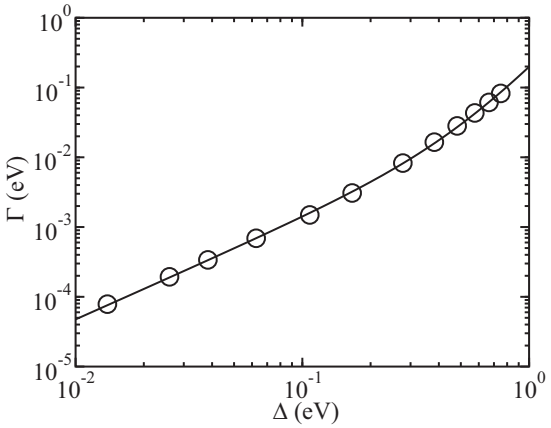

FIG. 4. The effective width Γ against effective resonance energy $\Delta(s_\varepsilon)$. The solid line is the fitted width (see the text for details).

waves reveals that the lowest three effective orbital angular momenta $\tilde{\ell}$ becomes 0.939, 2.01, and 3.02, respectively [56]. To include the contribution from the lowest three partial waves, the effective width is fitted as

$$\Gamma(\varepsilon) = \sum_i a_i \varepsilon^{\tilde{\ell}_i + 1/2}, \tag{19}$$

where $a_1 = 0.0356$, $a_2 = 0.0258$, and $a_3 = 0.137$. Near threshold, we then have $\Gamma(\varepsilon) \propto \varepsilon^{\tilde{\ell}+1/2} = \varepsilon^{1.439}$.

To calculate the cross section with the shifted anionic potential curve, we use the same effective width as a function of electron energy. This is justified because the electron energy is set to equal the resonance energy in our approach. As we offset the resonance energy, the effective width will be zero at the new crossing point between the shifted potential and the neutral potential. Therefore, the effective width is also shifted in terms of coordinate implicitly. In addition, the threshold behavior of the width changes only slightly as we shifted the anionic potential curve. Indeed, at $s_1 = -1.5$, the permanent dipole moment of H_2CN differs by only about 6% from the value at $s_1 = 1.25$. By fitting the effective width with new $\tilde{\ell}$, we found that the capture cross section also changes by about 6%.

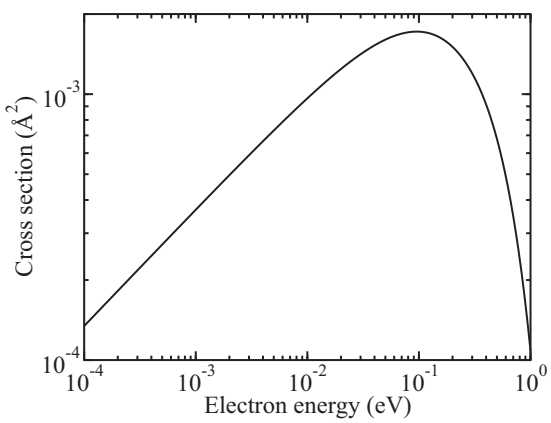

FIG. 5. Electron capture cross section for H_2CN.

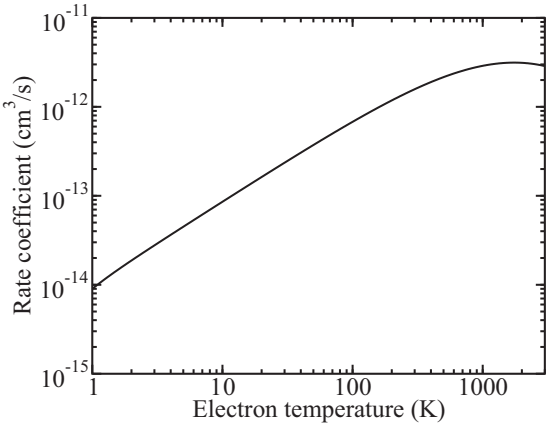

FIG. 6. Thermally averaged rate coefficient for electron capture by H_2CN (solid line) and its fit (dashed line, not distinguishable from the solid line).

Figure 5 displays the capture cross section versus electron energy. Near threshold, the cross section grows with electron energy as $\varepsilon^{0.439}$. The peak of the cross section is located near 0.1 eV. Around 1 meV, the cross section is about 3.68 $\times$ 10^{-20} cm^2, which is about 2 orders of magnitude larger than the cross section for the radiative electron attachment to CN [33].

Using the standard formula

$$k(T) = \frac{8\pi}{(2\pi k_b T)^{3/2}} \int \varepsilon\, \sigma(\varepsilon) e^{-\varepsilon/k_b T} d\varepsilon,$$

where k_b is the Boltzmann constant, we obtain the thermally averaged capture rate coefficient, which is shown in Fig. 6. The rate coefficient is fitted within 1% relative error using the form $k(T) = a_1 (T/300)^{a_2} e^{a_3 T^{a_4}}$, with $a_1 = 2.43 \times 10^{-12}$, $a_2 = 0.97025$, $a_3 = -9.20 \times 10^{-3}$, and $a_4 = 0.677$. The rate coefficient at 30 K is found to be about 2.36 $\times$ 10^{-13} cm^3/s, which is 2 orders larger than the REA of CN [33] and 1 order larger than the reaction of HCN + H^- [32]. Assuming the rate coefficient of electron capture is equal to the rate coefficient of forming CN^- by DEA and the ratio of H_2CN density to CN to be 1000 [36], we have

$$\frac{[e^-][\mathrm{CN}]k_{\mathrm{REA}}}{[e^-][\mathrm{H_2CN}]k_{\mathrm{DEA}}} \approx 10,$$

at 30 K, such that DEA of H_2CN is at least 10 times less efficient in producing CN^- than REA of CN. Hence, our result suggests that DEA of H_2CN may not play a major role in the formation of CN^- in the circumstellar envelope of IRC +10216. Other possible radicals that could produce CN^- by DEA in IRC +10216 are MgNC [57,58], MgCN [59], SiCN [60], SiNC [61], FeCN [62], and CCN [63], where all species have been detected in IRC +10216. It is possible that CN^- anions are produced by DEA of several of the above molecules efficiently in the inner region of the circumstellar envelope.

V. UNCERTAINTY ESTIMATION

As in many similar theoretical studies, there are two types of uncertainties [64]. One is related to the uncertainties of the theoretical model, and the second type is related to the choice

of parameters of the model (such as a limited basis set and uncertainties in *ab initio* or fitted data employed in the given model). In the present case, the main source of the first type of uncertainties is probably due to the reduced dimensionality approximation used in the present treatment and the neglect of the autodetachment process once the electron is captured into the dissociative coordinate. The uncertainties of the model can only be estimated if there is another more accurate model. For example, a fully dimensional time-dependent propagation model similar to that used in Ref. [3] could be used to benchmark the present results.

The evaluation of the second type of uncertainties is possible. The uncertainty of the cross section can be estimated by performing *R*-matrix calculations with various complete active spaces, *R*-matrix radii, and *R*-matrix basis sets. At equilibrium geometry, the position and width of the resonance differ, respectively, by at most 20% and 25% by varying the complete active space from 8 to 11 molecular orbitals and *R*-matrix radii from 10 to 14 bohrs with basis sets `cc-pVTZ` or `cc-pVQZ`. As a result, the capture cross section, which is proportional to the effective width, has associated uncertainty of about 25%.

Another source of uncertainty arises from the offset of the anionic potential energy. The relative error between the *ab initio* data used [45] and the experiment is about 2%. We found that changing the shifting by 2% leads to the change of cross section by about 7%. In the most unfortunate case, if we decrease the shift by 20%, the capture cross section increases by about a factor of 2. Therefore, our approach for H_2CN gives reasonable orders of magnitude of the capture cross section.

VI. CONCLUDING REMARKS

The approach presented in this article is based on the fact that, in general, the resonance energy varies substantially over only a subset of normal coordinates. As the resonance energy is nearly constant over H_2CN normal coordinates of the C_s symmetry, we expect our approach to work also for other polyatomic molecules. For instance, the DEA of acetylene starts with bending the molecule [3] such that the corresponding normal coordinate is responsible for the capture step in the process.

The present approach has several limitations: The survival probability is assumed to be unity. Therefore, our approach gives an upper bound of the DEA cross section within the Frank-Condon and WKB approximations. Also, the width is assumed to be on-shell, so that our approach would work only for systems with narrow resonances [55]. But if the width is narrow enough, the survival factor is closed to unity so that the two limitations are in fact equivalent. Finally, our approach cannot predict branching ratios of the dissociation products. By constructing a multidimensional anionic potential energy surface, it is possible to determine branching ratios by propagating wave packets. But this method is computationally expensive and will be reserved for future study.

To date, it is still a very challenging task to include the nonlocal operator to polyatomic molecules with several dissociation coordinates. Even for the local complex potential model, it is computationally demanding to compute resonance positions and widths at different geometries and perform time-dependent calculations. Besides, to obtain *ab initio* energy-dependent widths is difficult, even for diatomic molecules. Our approach can thus provide an *ab initio* estimation of the DEA cross section when other more accurate approaches are computationally expensive or unavailable.

ACKNOWLEDGMENT

This work was supported by the National Science Foundation through Grant No. PHY-1806915.

[1] R. Wilde, G. A. Gallup, and I. I. Fabrikant, J. Phys. B **33**, 5479 (2000).
[2] I. I. Fabrikant, H. Hotop, and M. Allan, Phys. Rev. A **71**, 022712 (2005).
[3] S. T. Chourou and A. E. Orel, Phys. Rev. A **77**, 042709 (2008).
[4] S. Chourou and A. E. Orel, J. Phys.: Conf. Ser. **300**, 012014 (2011).
[5] G. A. Gallup, P. D. Burrow, and I. I. Fabrikant, Phys. Rev. A **79**, 042701 (2009).
[6] K. Graupner, S. A. Haughey, T. A. Field, C. A. Mayhew, T. H. Hoffmann, O. May, J. Fedor, M. Allan, I. I. Fabrikant, E. Illenberger, M. Braun, M.-W. Ruf, and H. Hotop, J. Phys. Chem. A **114**, 1474 (2009).
[7] G. A. Gallup and I. I. Fabrikant, J. Chem. Phys. **135**, 134316 (2011).
[8] G. A. Gallup and I. I. Fabrikant, Phys. Rev. A **83**, 012706 (2011).
[9] M. Tarana, K. Houfek, J. Horáček, and I. I. Fabrikant, Phys. Rev. A **84**, 052717 (2011).
[10] T. N. Rescigno, C. S. Trevisan, A. E. Orel, D. S. Slaughter, H. Adaniya, A. Belkacem, M. Weyland, A. Dorn, and C. W. McCurdy, Phys. Rev. A **93**, 052704 (2016).
[11] M. Zawadzki, M. Čížek, K. Houfek, R. Čurík, M. Ferus, S. Civiš, J. Kočišek, and J. Fedor, Phys. Rev. Lett. **121**, 143402 (2018).
[12] I. I. Fabrikant, S. Eden, N. J. Mason, and J. Fedor, *Advances in Atomic, Molecular, and Optical Physics* (Elsevier, New York, 2017), Vol. 66, pp. 545–657.
[13] S. T. Chourou and A. E. Orel, Phys. Rev. A **80**, 032709 (2009).
[14] S. T. Chourou and A. E. Orel, Phys. Rev. A **83**, 032709 (2011).
[15] J. Royal and A. Orel, J. Chem. Phys. **125**, 214307 (2006).
[16] D. J. Haxton, Z. Zhang, H.-D. Meyer, T. N. Rescigno, and C. W. McCurdy, Phys. Rev. A **69**, 062714 (2004).
[17] D. J. Haxton, C. W. McCurdy, and T. N. Rescigno, Phys. Rev. A **75**, 012710 (2007).
[18] D. J. Haxton, T. N. Rescigno, and C. W. McCurdy, Phys. Rev. A **75**, 012711 (2007).
[19] D. J. Haxton, T. N. Rescigno, and C. W. McCurdy, Phys. Rev. A **78**, 040702(R) (2008).

[20] H. Adaniya, B. Rudek, T. Osipov, D. J. Haxton, T. Weber, T. N. Rescigno, C. W. McCurdy, and A. Belkacem, Phys. Rev. Lett. **103**, 233201 (2009).

[21] D. J. Haxton, H. Adaniya, D. S. Slaughter, B. Rudek, T. Osipov, T. Weber, T. N. Rescigno, C. W. McCurdy, and A. Belkacem, Phys. Rev. A **84**, 030701 (2011).

[22] D. S. Slaughter, H. Adaniya, T. N. Rescigno, D. J. Haxton, A. E. Orel, C. W. McCurdy, and A. Belkacem, J. Phys. B **44**, 205203 (2011).

[23] A. Moradmand, D. S. Slaughter, D. J. Haxton, T. N. Rescigno, C. W. McCurdy, Th. Weber, S. Matsika, A. L. Landers, A. Belkacem, and M. Fogle, Phys. Rev. A **88**, 032703 (2013).

[24] S. Petrie, Mon. Not. R. Astron. Soc. **281**, 137 (1996).

[25] E. Herbst and Y. Osamura, Astrophys. J. **679**, 1670 (2008).

[26] T. J. Millar, C. Walsh, and T. A. Field, Chem. Rev. **117**, 1765 (2017).

[27] T. F. O'Malley, Phys. Rev. **150**, 14 (1966).

[28] J. Bardsley, J. Phys. B **1**, 349 (1968).

[29] M. Agúndez, J. Cernicharo, M. Guélin, C. Kahane, E. Roueff, J. Klos, F. Aoiz, F. Lique, N. Marcelino, J. Goicoechea, M. González García, C. Gottlieb, M. McCarthy, and P. Thaddeus, Astron. Astrophys. **517**, L2 (2010).

[30] B. Eichelberger, T. P. Snow, C. Barckholtz, and V. M. Bierbaum, Astrophys. J. **667**, 1283 (2007).

[31] M. Cordiner and T. Millar, Astrophys. J. **697**, 68 (2009).

[32] M. Satta, F. Gianturco, F. Carelli, and R. Wester, Astrophys. J. **799**, 228 (2015).

[33] N. Douguet, S. Fonseca dos Santos, M. Raoult, O. Dulieu, A. E. Orel, and V. Kokoouline, Phys. Rev. A **88**, 052710 (2013).

[34] M. Ohishi, D. McGonagle, W. M. Irvine, S. Yamamoto, and S. Saito, Astrophys. J. **427**, L51 (1994).

[35] T. J. Millar and E. Herbst, Astron. Astrophys. **288**, 561 (1994).

[36] T. Millar, E. Herbst, and R. Bettens, Mon. Not. R. Astron. Soc. **316**, 195 (2000).

[37] H.-J. Werner, P. J. Knowles, R. Lindh, F. R. Manby, M. Schütz *et al.*, MOLPRO, vers. 2008.3, a package of *ab initio* programs (2008).

[38] P. J. Knowles and H.-J. Werner, Chem. Phys. Lett. **145**, 514 (1988).

[39] H.-J. Werner and P. J. Knowles, J. Chem. Phys. **89**, 5803 (1988).

[40] T. H. Dunning, Jr., J. Chem. Phys. **90**, 1007 (1989).

[41] A. E. Wiens, A. V. Copan, E. C. Rossomme, G. J. Aroeira, O. M. Bernstein, J. Agarwal, and H. F. Schaefer, J. Chem. Phys. **148**, 014305 (2018).

[42] M. E. Jacox, J. Phys. Chem. **91**, 6595 (1987).

[43] D. C. Cowles, M. J. Travers, J. L. Frueh, and G. B. Ellison, J. Chem. Phys. **94**, 3517 (1991).

[44] N. R. Brinkmann, S. S. Wesolowski, and H. F. Schaefer III, J. Chem. Phys. **114**, 3055 (2001).

[45] W. Eisfeld, J. Chem. Phys. **120**, 6056 (2004).

[46] V. Barone, P. Carbonniere, and C. Pouchan, J. Chem. Phys. **122**, 224308 (2005).

[47] C. Puzzarini and V. Barone, Chem. Phys. Lett. **467**, 276 (2009).

[48] C. Puzzarini, M. Biczysko, and V. Barone, J. Chem. Theory Comput. **6**, 828 (2010).

[49] J. Tennyson, Phys. Rep. **491**, 29 (2010).

[50] J. Carr, P. Galiatsatos, J. Gorfinkiel, A. Harvey, M. Lysaght, D. Madden, Z. Mašín, M. Plummer, J. Tennyson, and H. Varambhia, Euro. Phys. J. D **66**, 58 (2012).

[51] J. Tennyson, D. B. Brown, J. J. Munro, I. Rozum, H. N. Varambhia, and N. Vinci, J. Phys.: Conf. Ser. **86**, 012001 (2007).

[52] J. Tennyson and C. J. Noble, Comput. Phys. Commun. **33**, 421 (1984).

[53] K. Wang, Y. An, J. Meng, Y. Liu, and J. Sun, Phys. Rev. A **89**, 022711 (2014).

[54] W. Domcke, Phys. Rep. **208**, 97 (1991).

[55] I. I. Fabrikant, Phys. Rev. A **94**, 052707 (2016).

[56] N. Douguet, V. Kokoouline, and C. H. Greene, Phys. Rev. A **80**, 062712 (2009).

[57] K. Kawaguchi, E. Kagi, T. Hirano, S. Takano, and S. Saito, Astrophys. J. **406**, L39 (1993).

[58] M. Guélin, R. Lucas, and J. Cernicharo, Astron. Astrophys. **280**, L19 (1993).

[59] L. Ziurys, A. Apponi, M. Guélin, and J. Cernicharo, Astrophys. J. **445**, L47 (1995).

[60] M. Guélin, S. Muller, J. Cernicharo, A. Apponi, M. McCarthy, C. Gottlieb, and P. Thaddeus, Astron. Astrophys. **363**, L9 (2000).

[61] M. Guélin, S. Muller, J. Cernicharo, M. McCarthy, and P. Thaddeus, Astron. Astrophys. **426**, L49 (2004).

[62] L. Zack, D. Halfen, and L. M. Ziurys, Astrophys. J. Lett. **733**, L36 (2011).

[63] J. Anderson and L. M. Ziurys, Astrophys. J. Lett. **795**, L1 (2014).

[64] H.-K. Chung, B. Braams, K. Bartschat, A. Csaszar, G. Drake, T. Kirchner, V. Kokoouline, and J. Tennyson, J. Phys. D: Appl. Phys. **49**, 363002 (2016).